1 **Using Satellite Measurements of N$_2$O to remove dynamical variability from HCl**
2 **measurements**

4 Richard S. Stolarski
5 Johns Hopkins University
6
7 Anne R. Douglass, Susan E. Strahan
8 NASA Goddard Space Flight Center

10 *Abstract:*
11

12 Column HCl measurements show deviations from the expected slow decline
13 following the regulation of chlorine-containing compounds by the Montreal Protocol.
14 We use the simultaneous measurements of N$_2$O and HCl by the MLS instrument on
15 the Aura satellite to examine this problem. We find that the use of N$_2$O
16 measurements at a specific altitude to represent the impact of dynamical variability
17 on HCl results in a derived linear trend in HCl that is negative (ranging from -
18 2.5%/decade to 5.3%/decade) at all altitudes between 68 hPa and 10 hPa. These
19 trends are at or near 2σ statistically significance at all pressure levels between 68
20 hPa and 10 hPa.

21
22 **I. Introduction**
23
24 HCl is the primary constituent of inorganic chlorine in the stratosphere, comprising
25 75-80% of the inorganic chlorine in the altitude range from 68 hPa to 10 hPa
26 [Zander et al., 1992; Nassar, et al. 2006]. As such it provides a convenient marker
27 for the total amount of inorganic stratospheric chlorine that can be measured from
28 the ground and from satellites. The column amount of HCl is expected to follow the
29 behavior of the concentration of the organic sources of chlorine as measured at the
30 surface (e.g. CFCs) with a time delay of a few years for the CFCs to reach the
31 stratosphere where they are converted to inorganic chlorine compounds.
32
33 Rinsland et al. [2003] showed from ground-based measurements that the amount
34 inorganic chlorine (HCl + ClONO$_2$) in the stratosphere leveled out using data
35 through 2002. The next step would be to observe the expected decrease in
36 inorganic chlorine. Recently Mahieu et al. [2014] have shown that, in fact, the
37 measured HCl column over Jungrfraujoch decreased more rapidly than expected
38 from ground-based measurements of source gases during the early 2000's followed
39 by an increase from about 2007 to 2010. We show that the Microwave Limb
40 Sounder (MLS) measurements of the lower stratospheric column of HCl also
41 decrease and increase in concert with the Jungfraujoch data, followed by a decrease
42 from 2011 to mid 2013 and a subsequent increase from that time to the present (see
43 Figure 1).
44
45
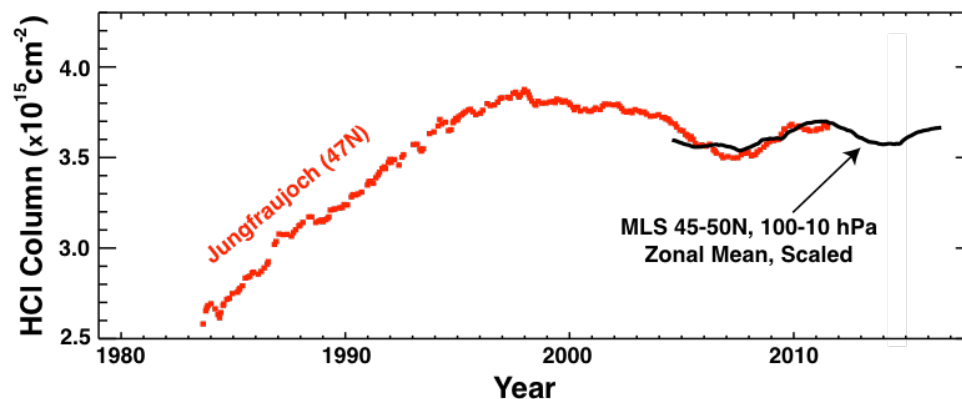
2
3 Figure 1: Total column measurements of HCl above Jungfraujoch smoothed with a 3-year
4 running mean as shown by Mahieu et al. [2014] (red curve). Also shown are the 3-year
5 running mean smoothed zonal mean of measurements of the lower stratospheric column of
6 HCl (100-10 hPa) from the MLS instrument on Aura for the latitude band from 45 to 50N
7 (black curve). The MLS measurements are of partial column and have been scaled upward
8 to match the Jungfraujoch FTIR measurements for better visual comparison.
9
10 Mahieu et al. [2014] use results from model simulations with SLIMCAT driven by
11 ERA-Interim meteorological fields from the European Centre for Medium-Range
12 Weather Forecasts (ECMWF) to suggest that variability in the stratospheric
13 circulation causes the accelerated decrease and the unexpected increase in HCl
14 column. We will explore this explanation using measurements of N_2O from MLS as a
15 measure of this variability in circulation.
16
17 **2. MLS Data: HCl and N_2O**
18
19 We will use the MLS HCl data to test whether chlorine is decreasing in the
20 stratosphere as expected from adherence to the provisions of the Montreal Protocol.
21 MLS was launched on the Aura Satellite in late 2004 [Waters et al., 2006] and
22 continues to operate in 2017. The record is now more than 13 years in length with
23 altitude profiles of HCl, HNO_3, N_2O and many other species measured globally on a
24 daily basis.
25
26 For HCl we use the version 4.2 product that has little change since the previous
27 version 3 products. According to the MLS data quality document [Livesey et al.,
28 2017] the useful range for HCl measurements is from 100 to 0.32 hPa. However, the
29 useful data for trends is limited to pressures greater than 10 hPa due to the
30 insufficient reliability of the band 14 retrievals in the upper stratosphere.
31
32 For N_2O we use the version 4.2 redefined standard product that uses signals from
33 the band 3 (190-GHz channel); the standard product was redefined because the
34 product from band 12 (640 GHz channel) deteriorated and the band was shut off in

1   August 2013. In the next section we will compare this redefined standard to the
2   measurements from the 640-GHz channel and correct for the drift observed
3   between these two channels during the time that both were yielding N_2O
4   measurements. The 190-GHz N_2O data are stated to be useful in the 68-0.46 hPa
5   range. We will thus restrict our analyses to pressure levels between 68 and 10 hPa
6   in this paper where both the HCl and N_2O measurements are useful.
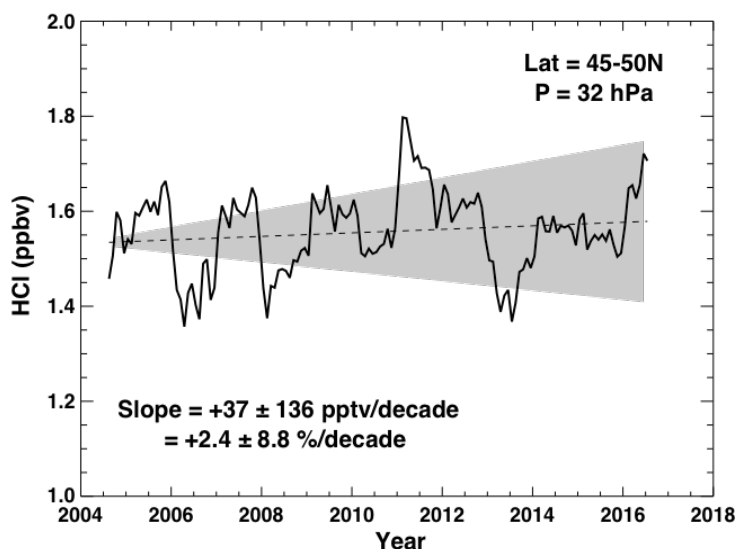
9   Figure 2: Deseasonalized monthly-mean MLS measurements of HCl concentration at 32 hPa.
10   Measurements are area-weighted between 45°N and 50°N. The heavy dashed line is a
11   linear least squares fit to the data and the shaded area indicates the 2σ uncertainty in that
12   fit including consideration of auto-correlation in the time series.
13
14   To better understand the variations in HCl column amounts at 47°N observed by
15   Mahieu et al. [2014] we begin with consideration of the MLS measurements of the
16   HCl profile at specific pressure levels in the stratosphere. For example, Figure 2
17   shows the anomalies in the MLS monthly-mean measurements of HCl averaged
18   between 45°N and 50°N latitude at the 32 hPa pressure level. The data are shown in
19   percentage deviation from the seasonal mean of the entire data set. The data clearly
20   show deviations of as much as ±10% with significant auto-correlation.
21
22   One way to look at the HCl anomalies shown in Figure 2 is to attempt to "explain"
23   the variance by fitting to various measures of dynamical variability such as the
24   Quasi-Biennial Oscillation (QBO) or El-Niño/Southern Oscillation (ENSO). This
25   method may remove much of the dynamical variance but has at least two potential
26   problems: 1) the fitting parameters may only remove part of the dynamical
27   variability because of incomplete representation of that variability and 2) they may
28   over-represent the variability because of correlation between parameters. Either of

1   these problems could lead to difficulties in separating real trends from apparent
2   trends in the residual over short time scales such as the 12 years of data since 2004.
3   For example, the impact of the QBO on southern mid-latitude composition depends
4   on the QBO phase during early (southern) winter [Strahan et al. 2015]. The
5   resulting dynamical variability is not easily represented by fitting a QBO plus a
6   seasonal term in a statistical model, because the actual variability depends on an
7   interaction between the two effects.
8
9   We use a different method to remove dynamical variability in the HCl data set,
10 taking advantage of simultaneous measurements of another species made by the
11 MLS instrument on the Aura satellite. The observed anomalies are the result of
12 dynamical variability acting on mixing ratio gradients. These gradients may be
13 vertical, horizontal, or a combination of both. If two constituents have gradients in
14 the same or opposite directions, the impact of dynamic variability will be to cause
15 deviations, or anomalies, that are either correlated or anti-correlated depending on
16 the sign of the gradients. An example is shown in Figure 3 where we plot the
17 deseasonalized HCl mixing ratios at 32 hPa for the latitude band 45-50N as in Figure
18 2 and the deseasonalized N_2O mixing ratios on a reverse scale from MLS
19 measurements for the same latitude band and pressure level. The correlation
20 coefficient is -0.87 between these two anomaly time series. A similar correlation is
21 found between HCl and HNO_3 data from MLS.
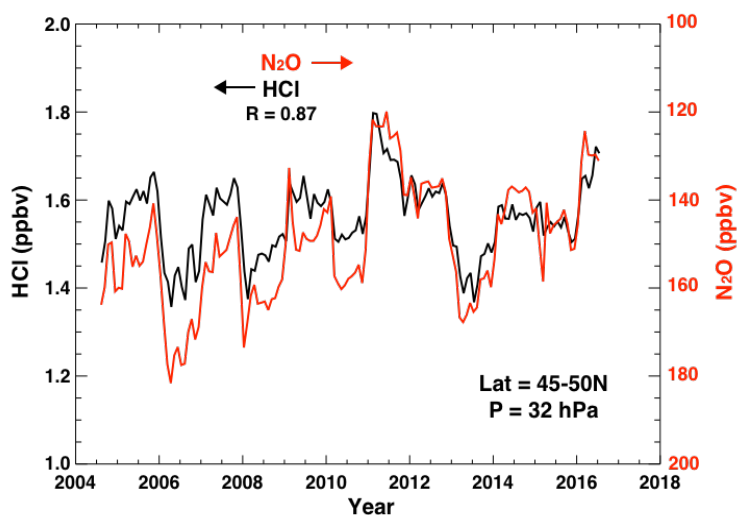
22
23 Figure 3: Deseasonalized time series of HCl (black curve, same as Figure 2) and
24 deseasonlized time series of N_2O plotted with reverse scale on right side of figure(red
25 curve) for the latitude band 45-50N at 32 hPa pressure level from MLS measurements of
26 each constituent.
27
28 **3. Time Series Analysis: Using N_2O Anomalies as a Fitting Parameter**
29

1 The trend that we are trying to isolate and confirm for the HCl time series is
2 determined by the change in abundance of chlorine-containing halocarbons driven
3 by the provisions of the Montreal Protocol on ozone-depleting substances. The
4 chlorine-containing source gases are expected to have decreased since 2000 in
5 response to the decreases in the chlorine-containing source gases. N_2O, on the other
6 hand, is known to be increasing at a rate of about 2.8%/decade [NOAA GMDL data
7 updated from Elkins and Dutton [2009] available at
8 ftp://ftp.cmdl.noaa.gov/hats/n2o/combined/HATS_global_N2O.txt]. Our approach
9 is to use the N_2O time series at each altitude, such as that shown in Figure 3, as an
10 explanatory variable in a time-series regression to remove the dynamical variability
11 from the HCl time series. Trends calculated for HCl in this time-series regression
12 are then corrected for the underlying trend in N_2O.
13
14
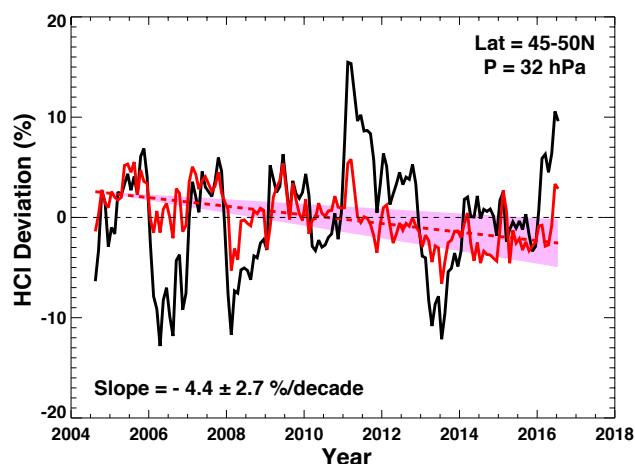
15
16 Figure 4: HCl anomaly time series as in Figures 2 and 3 (black) with residual time series
17 after fit to N_2O time series (red). Red dashed line is linear fit to residual series with 2σ
18 uncertainty bounds indicated by shaded area.
19
20 The result of using N_2O as a fitting parameter for the 32 hPa MLS time series for HCl
21 is shown in Figure 4. The solid red line in the figure is the residual time series after
22 fitting, which takes advantage of the substantial covariance and shows significantly
23 reduced variability. The resulting trend is shown by the red dashed line that has a
24 slope of – 4.4 ± 2.7 (2σ) %/decade. The HCl trend at this pressure level is now
25 negative and statistically significant at more than the 3σ level. The same procedure
26 has been carried out at each of the pressure levels for MLS retrievals. The result is
27 shown the third column of Table 1.
28
29 The second column of Table 1 shows the raw trend obtained from the MLS HCl
30 measurements. We can see that the raw trend is essentially the same as the N_2O-
31 fitted trend at the two highest levels (10 and 15 hPa) where dynamical variability is

1   relatively small. The trend at the lower levels is substantially different when using
2   N_2O as a fitting parameter. Using N_2O as a fitting parameter changes the lower level
3   trends from positive to negative with a substantial reduction in the uncertainty.
4
5   A further problem alluded to earlier in this section is that MLS now uses the 190-
6   GHz band for its standard N_2O product because the 640-GHz band is no longer
7   usable. The problem arises because the 190-GHz band displays a drift in N_2O
8   measurements with respect to the 640-GHz band [N. Livesey, pers. commun.]. Since
9   the 640-GHz band was found to be stable during its operational period, we use the
10   drift rate of the 190-GHz band with respect to the 640-GHz band calculated by the
11   MLS team for the time period in which they both were operational (2004-2012).
12   The results are shown in the fourth column of Table 1 with estimated uncertainties
13   in the fit.
14

Pressure Level (hPa)	Raw HCl Trend (%/dec)	Trend with N_2O fit (%/dec)	N_2O 190/640 drift (%/dec)	Surf N_2O Trend (%/dec)	Final HCl Trend (%/dec)
10	-3.7±2.0	-3.0±2.0	-5.1±3.7	+2.8±0.05	-5.3±4.2
15	-3.8±3.1	-3.5±1.9	-2.9±2.2	+2.8±0.05	-3.6±2.9
22	-1.3±4.2	-3.8±2.3	-1.5±1.3	+2.8±0.05	-2.5±2.6
32	+2,4±8.8	-4.4±2.7	-2.2±1.4	+2.8±0.05	-3.8±3.0
46	+3.8±7.2	-2.3±2.3	-5.2±1.8	+2.8±0.05	-4.7±2.9
68	+3.9±4.0	-1.3±2.7	-5.0±1.6	+2.8±0.05	-3.5±3.1

15
16   Table 1. HCl trends derived from MLS data at 6 pressure levels. Column 1 gives the
17   pressure level. Column 2 gives the raw trend derived directly from the MLS HCl
18   measurements in %/decade with 2σ uncertainties. Column 3 gives the HCl trend derived
19   using MLS N_2O measurements as an explanatory variable. Column 4 gives the derived trend
20   in the 190-GHz channel of MLS N_2O measurements relative to the 640-GHz channel during
21   the time of their overlap. Column 5 gives the slope of the NOAA global surface
22   measurements of N_2O over the period from 2001 to 2012. Column 6 gives the overall
23   resulting trend obtained by combining the information in columns 3 to 5.
24
25   Finally, we note that the surface levels of N_2O increased by about 2.8%/decade. We
26   used the "global" nitrous oxide data reported at the NOAA ESRL Global Monitoring
27   Division web site (https://www.esrl.noaa.gov/gmd/hats/combined/N2O.html). We
28   fit a trend to the data between 2001 and 2012 to represent the ground values that
29   should be seen in the stratosphere about 3 years later in the MLS data. The time
30   delay represents the approximate mean age of air in the lower stratosphere.
31
32   The final result is obtained by summing the trends in columns 3 to 5 of Table 1 and
33   is shown in column 6 of the table. The uncertainties were obtained by using the root
34   sum of squares (RSS) of the uncertainties in columns 3 to 5. This final result is also
35   shown in Figure 5. The blue solid line indicates the trend result obtained from a
36   linear fit to the deseasonalized residuals with no attempt to account for dynamical
37   variability (column 2 of Table 1). The red solid curve is the result when the N_2O

1 time series is used as a dynamical surrogate, with corrections for drift and surface
2 trends, in the fitting procedure (column 6 of Table 1). The shaded areas represent
3 2σ uncertainties in the linear trends.
4
5 Note in Figure 5 that the use of N$_2$O as a surrogate for dynamical variability reduces
6 the uncertainty in the calculated trend for all of the pressure levels between 15 hPa
7 and 68 hPa where the MLS data for both HCl and N$_2$O are considered to be good for
8 trend analysis. Figure 5 also shows that the calculated linear trend in HCl using the
9 N$_2$O surrogate with corrections is negative at all pressure levels and is significantly
10 negative (2σ) at all levels from 68 hPa to 10 hPa with the exception of 22 hPa where
11 it has nearly 2σ significance.
12
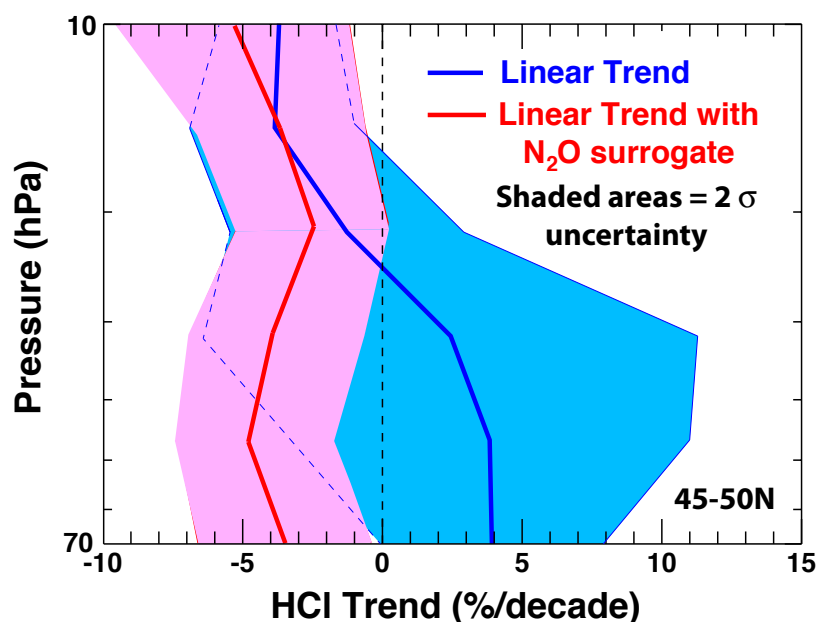
13
14 Figure 5: Linear trend in HCl concentrations determined from MLS measurements between
15 70 and 10 hPa for the latitude band of 45-50N. The blue line is the trend determined from
16 the raw deseasonalized data. The red curve is the trend determined while including the N$_2$O
17 time series as an explanatory variable. The shaded areas represent 2σ uncertainties for
18 each.
19
20
21 **4. Conclusion**
22
23 In their paper, Mahieu et al. [2014] showed that total column HCl measured at
24 Jungfraujoch showed significant variation from the expected simple linear trend.
25 We have attempted to quantitatively evaluate the effect of dynamical variability on
26 the concentrations of HCl in the stratosphere by using N$_2$O measurements since late

1   2004 made by the Aura MLS instrument. Since both HCl and N_2O have
2   concentration gradients (horizontal and vertical) that are acted upon by dynamical
3   processes to create inter-annual variability, we have used the variability of N_2O
4   concentrations determined from MLS observations as a measure of the dynamical
5   variability that should be expected in HCl concentrations. We suggest that this
6   method more reliably removes the real atmospheric variability than does the use of
7   other proxies.
8
9   We have shown that using an N_2O surrogate in trend analysis of the MLS HCl time
10 series results in a trend that is negative at all measured levels from 68 hPa upward
11 to 10 hPa and that these negative trends are 2σ statistically significant or nearly so.
12 The N_2O surrogate had little effect at the upper two levels of 10 and 15 hPa where
13 the dynamical variability is less significant. The surrogate had significant impact on
14 the derived trends lower in the stratosphere where most of the HCl column resides.
15
16 Previous data-based estimates of HCl decrease in the stratosphere include
17 Froidevaux et al. [2006], Jones et al. [2011], Brown et al. [2011], and Kohlhepp et al.
18 [2012]. All of these studies had to consider the issues we have discussed in this
19 paper, namely the contribution of dynamic variability to the apparent trend. In each
20 case, the shortness of the data record was a significant limitation to the
21 interpretation of potential trends due to the decrease in tropospheric organic
22 chlorine sources.
23
24 The results from these authors are summarized in the 2014 Ozone Assessment
25 Report [Carpenter and Reimann, 2015]. Specifically Froidevaux et al. [2006]
26 derived a trend for the 50-65 km altitude range of -8%/decade from MLS data for
27 the years 2004-2006. Jones et al. [2011] derived a trend of -5%/decade using
28 HALOE and ACE FTS data between 35 and 45 km from 1997 to 2008 at midlatitudes.
29 Brown et al. [2011] deduced a trend of -7%/decade for the 50 to 54 kkm range from
30 ACE FTS data from 2004 to 2010. Finally, Kohlhepp et al. [2012] analyzed the total
31 column HCl data from 17 NDACC FTIR stations for the years 2000 to 2009, obtaining
32 trends that ranged from -4 to -16%/decade depending on station.
33
34 The best comparison for evaluating our results is considering the change in the
35 organic chlorine sources at the surface. The 2014 ozone assessment, Chapter 1,
36 [Carpenter and Reimann, 2015] estimates changes in the tropospheric available
37 organic chlorine of -6%/decade from 2000-2004 followed by -4.6%/decade from
38 2004-2008 and -4%/decade from 2008-2012. Assuming a 3-5 year delay between
39 changes in the tropospheric source gases for the stratospheric chlorine implies an
40 average change from 2004 to 2016 of about -4.9%/decade, in agreement with our
41 estimate from MLS data within the uncertainty bounds.
42
43
44
45

2 **References:**
3
4 Brown, A.T., M.P. Chipperfield, C. Boone, C. Wilson, K.A. Walker, and P.F. Bernath,
5   [2011], Trends in atmospheric halogen containing gases since 2004, *J. Quant.*
6   *Spectrosc. Raiat. Transfer*, *112* (16), 2552-2566, doi:
7   10.1016/j.jqsrt.2011.07.005.
8 Carpenter, L.J. and S. Reimann [2015], Lead Authors, Scientific Assessment of Ozone
9   Depletion: 2014, Chapter 1: Update on Ozone-Depleting Substances (ODSs)
10   and Other Gases of Interest to the Montreal Protocol
11   Global Ozone Research and Monitoring Project—Report No. 55.
12
13 Elkins, J.W, and G.S. Dutton [2009], Nitrous oxide and sulfur hexafluoride [in 'State
14   of the Climate in 2008']. *Bull. Amer. Meteor. Soc*, 90 S38-S39.
15
16 Froidevaux, L., N.J. Livesey, W.G. Read, R.J. Salawitch, J.W. Waters, B. Drouin, I.A.
17   MacKenzie, H.C. Pumphrey, P. Bernath, C. Boone, R. Nassar, S. Montzka, J.
18   Elkins, D. Cunnold, and D. Waugh [2006], Temporal decrease in upper
19   atmospheric chlorine, *Geophys. Res. Lett.*, *33*, L23812, doi:
20   10.1029/2006GL027600
21
22 Jones, A., J. Urban, D.P. Murtagh, C. Sanchez, K.A. Walker, N.J. Livesey, L. Froidevaux,
23   and M.L. Santee [2011], Analysis of HCl and ClO time series in the upper
24   stratosphere using satellite data sets, *Atmos. Chem. Phys.*, *11* (11), 5321-5333,
25   doi: 10.5194/acp-11-5321-2011
26
27
28 Kohlhepp, R., R. Ruhnke, M.P. Chipperfield, M. De Maziere, J. Notholt, S. Barthlott, R.L.
29   Batchelor, R.D. Blatherwick, T. Blumenstock, M.T. Coffey, P. Demoulin, H. Fast,
30   W. Feng, A. Goldman, D.W.T. Griffith, K. Hamann, J.W. Hannigan, F. Hase, N.B.
31   Jones, A. Kagawa, I. Kaiser, Y. Kasai, O. Kirner, W. Kouker, R. Lindenmaier, E.
32   Mahieu, R.L. Mittermeier, B. Monge-Sanz, I. Morino, I. Murata, H. Nakajima, M.
33   Palm, C. Paton-Walsh, U. Raffalski, T. Reddmann, M. Rettinger, C.P. Rinsland, E.
34   Rozanov, M. Schneider, C. Senten, C. Servais, B.-M. Sinnhuber, D. Smale, K.
35   Strong, R. Sussmann, J.R. Taylor, G. Vanhaelewyn, T. Warneke, C. Whaley, M.
36   Wiehle, and S.W. Wood [2012], Observed and simulated time evolution of HCl,
37   ClONO2, and HF total column abundances, *Atmos. Chem. Phys.*, *12* (7), 3527-
38   3556, doi: 10.5194/acp-12-3527-2012,
39
40 Livesey, Nathaniel J., William G. Read, Paul A. Wagner, Lucien Froidevaux, Alyn
41   Lambert, Gloria L. Manney, Luis F. Milla´n Valle, Hugh C. Pumphrey, Michelle
42   L. Santee, Michael J. Schwartz, Shuhui Wang, Ryan A. Fuller, Robert F. Jarnot,
43   Brian W. Knosp, Elmain Martinez [2017], Jet Propulsion Laboratory Report
44   JPL D-33509 Rev. B, "Earth Observing System (EOS) Aura Microwave Limb
45   Sounder (MLS) Version 4.2x-3.0: Level 2 data quality and description
46   document".

2   Mahieu, E., M.P. Chipperfield, J. Notholt, T. Reddmann, J. Anderson, P.F. Bernath, T.
3   Blumenstock, M.T. Coffey, S.S. Dhomse, W. Feng, B. Franco, L. Froidevaux, D.W.
4   T. Griffith, J.W. Hannigan, F. Hase, R. Hossaini, N.B. Jones, I. Morino, I. Murata,
5   H. Nakajima, M. Palm, C. Paton-Walsh, J.M. Russell III, M. Schneider, C. Servais,
6   D. Smale, and K.A. Walker [2014], Recent Northern Hemisphere stratospheric
7   HCl increase due to atmospheric circulation changes, Nature, 515, 104-107,
8   doi=10.1038/nature13857.
9
10   Nassar, R., P. F. Bernath, C. D. Boone, C. Clerbaux, P. F. Coheur, G. Dufour, L.
11   Froidevaux, E. Mahieu, J. C. McConnell, S. D. McLeod, D. P. Murtagh,
12   C. P. Rinsland, K. Semeniuk, R. Skelton, K. A. Walker, and R. Zander [2006], A
13   global inventory of stratospheric chlorine in 2004, J. Geophys. Res. 111,
14   D22312, doi:10.1029/2006JD007073.
15
16   Rinsland, C. P., et al. [2003], Long-term trends of inorganic chlorine from ground-
17   based infrared solar spectra: Past increases and evidence for stabilization, J.
18   Geophys. Res., 108 (D8), 4252, doi:10.1029/2002JD003001, 2003.
19
20   Strahan, S. E., L. D. Oman, A. R. Douglass, and L. Coy (2015), Modulation of Antarctic
21   vortex composition by the quasi-biennial oscillation, Geophys. Res. Lett., 42,
22   doi:10.1002/2015GL063759.
23
24   Waters, J.W., L. Froidevaux, R.S. Harwood, R.F. Jarnot, H.M. Pickett, W.G. Read, P.H.
25   Siegel, R.E. Cofield, M.J. Filipiak, D.A. Flower, J.R. Holden, G.K. Lau, N.J. Livesey,
26   G.L. Manney, H.C. Pumphrey, M.L. Santee, D.L. Wu, D.T. Cuddy, R.R. Lay, M.S.
27   Loo, V.S. Perun, M.J. Schwartz, P.C. Stek, R.P. Thurstans, M.A. Boyles, S.
28   Chandra, M.C. Chavez, G-S. Chen, B.V. Chudasama, R. Dodge, R.A. Fuller, M.A.
29   Girard, J.H. Jiang, Y. Jiang, B.W. Knosp, R.C. LaBelle, J.C. Lam, K.A. Lee, D. Miller,
30   J.E. Oswald, N.C. Patel, D.M. Pukala, O. Quintero, D.M. Scaff, W.V. Snyder, M.C.
31   Tope, P.A. Wagner, and M.J. Walch (2006), The Earth Observing System
32   Microwave Limb Sounder (EOS MLS) on the Aura satellite, IEEE Trans. Geosci.
33   Remote Sensing 44, no. 5, doi:10.1109/TGRS.2006.873771.
34
35   Zander, R., M.R. Gunson, C.B. Farmer, C.P. Rinsland, F.W. Irion, and E. Mahieu [1992],
36   The 1985 chlorine and fluorine inventories in the stratosphere based on
37   ATMOS observations at 30-degrees north latitude, J. Atmos. Chem. 15, 171-
38   186.
39
40
41
42